TECHNICAL TRANSACTIONS | **CZASOPISMO TECHNICZNE**
ENVIRONMENT ENGINEERING | ŚRODOWISKO
1-Ś/2013

PAWEŁ KISIEL, ARKADIUSZ KWIECIEŃ*

NUMERICAL ANALYSIS OF A POLYMER FLEXIBLE JOINT IN A TENSILE TEST

ANALIZA NUMERYCZNA POLIMEROWYCH ZŁĄCZY PODATNYCH PODDANYCH ROZCIĄGANIU

A b s t r a c t

The paper presents an analysis of Polymer Flexible Joint behaviour in a tensile test. Three Finite Element Method models have been developed in order to compare numerical and laboratory test results. A discrepancy between laboratory test results and computational results obtained in models based on material parameters derived from polymer dumbbell test has been shown. This work also presents the influence of the choice of hyperelastic material model on calculations accuracy in Polymer Flexible Joint analysis.

Keywords: hyperelasticity, parameters identification, polymer flexible joint, tensile test

S t r e s z c z e n i e

W artykule przedstawione zostały wyniki analizy pracy Polimerowego Złącza Podatnego poddanego rozciąganiu. Wykonano trzy modele rozciąganego złącza za pomocą Metody Elementów Skończonych oraz porównano uzyskane wyniki numeryczne z rezultatami badań eksperymentalnych. Praca prezentuje rozbieżności pomiędzy wynikami bazującymi na parametrach materiałowych z jednoosiowego rozciągania próbki polimeru a wynikami z eksperymentów laboratoryjnych. W pracy przedstawiono również wpływ doboru modelu hipersprężystego na rozbieżności wyników obliczeń i testów laboratoryjnych.

Słowa kluczowe: hipersprężystość, identyfikacja, polimerowe złącza podatne, rozciąganie

* M.Sc. Paweł Kisiel, Ph.D., D.Sc. Arkadiusz Kwiecień, Institute of Structural Mechanics, Faculty of Civil Engineering, Cracow University of Technology.

1. Introduction

Polymer Flexible Joint (PFJ) technology is an innovative technology which allows for the carrying of loads with large deformations [1]. In particular, the PFJ can be used as a repair technology suitable for historic structures, for buildings located in seismic areas or to join concrete slabs in airfield pavements [2].

The development of guidelines for PFJ numerical modelling is a very important aspect of technology improvement. Consequently, there has been made an attempt to determine the material model for PFJ in tensile tests. There were obtained parameters for Mooney-Rivlin material model, representing polymer in joints basing on uniaxial test data. However, after numerical calculations performance of flexible joints with particular dimensions, there has been shown, that there is a significant discrepancy between calculated results and those obtained by an experiment, this can be observed in Fig. 1 [3].

The aim of this work is to analyse flexible joint behaviour under a tensile load, taking into account different specimens' geometry and various material models. The parameters of material are derived from the uniaxial polymer dumbbell test and they are identified for four different hyperelastic models. The results presented below clearly show that none of the material models correctly fits the PFJ behaviour in the tensile test.

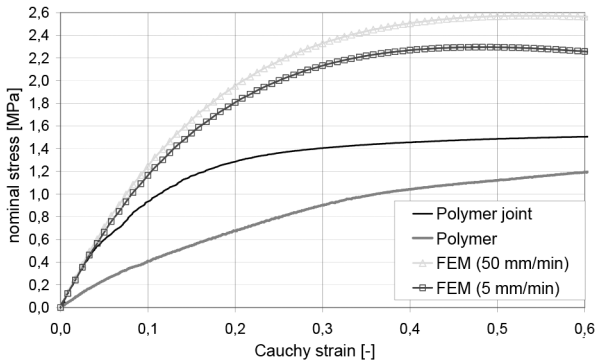

Fig. 1. Comparison of PFJ tensile laboratory test and numerical experiment results [3]

2. Description of experimental laboratory tests

Uniaxial tension tests were performed on 4 different types of specimens. First type was made of the PM-type polymer in a dumbbell shape, the other three types represent PFJ. Tests on the dumbbell shape specimens were performed according to [4]. Every specimen of PFJ consists of two concrete elements joined by a polymer layer. Schematic drawings of PFJ specimens are presented in Fig. 2. Tests on the PFJ specimens were performed according to own procedure.

Each concrete specimen was initially tested in the tensile test without the polymer layer to obtain correct data for numerical analysis. Subsequently, the test was performed for the PFJ specimens. The tensile tests were carried on ZWICK 1455 testing machine with maximum

force of 20 kN and precision of 0.1 N. There was used a mechanical extensometer of 0.005 mm precision. The tests were performed with displacement control of constant ratio of 50 mm/min. Sketch of the PFJ sample specimens are presented in Fig. 3.

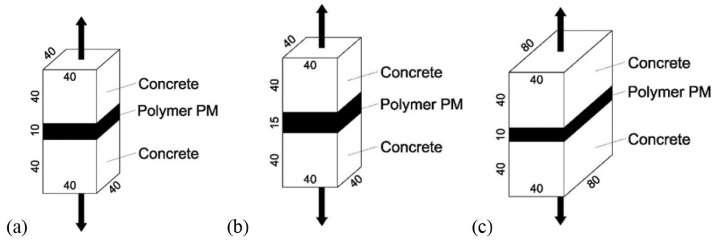

Fig. 2. Sketch of PFJ specimens with polymer joint dimensions: 40 × 40 × 10 (a), 40 × 40 × 15 (b) and 80 × 40 × 10 (c)

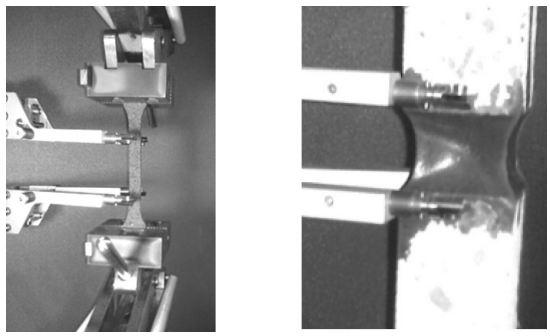

Fig. 3. Laboratory tests of polymer dumbbell specimens (on the left) and laboratory testes of PFJ (on the right)

3. Material parameters' identification

Material parameters identification has been performed basing on the Abaqus CAE 6.12 material property module. Tests data used for identification were obtained from the dumbbell tensile tests. There have been determined four different hyperelastic material models parameters. There are presented below analytical formulas for each applied material model.

– Mooney-Rivlin form – formula (1):

$$U = C_{10}\left(\overline{I}_1 - 3\right) + C_{01}\left(\overline{I}_2 - 3\right) + \frac{1}{D_1}(J^{el} - 1)^2 \tag{1}$$

where:

U – the strain energy per unit of reference volume,

C_{ij}, D_i – temperature-dependent material parameters;

$\overline{I}_1$ $\overline{I}_2$ – the first and second deviatoric strain invariants defined in formulae (2) and (3).

$$\overline{I}_1 = \overline{\lambda}_1^2 + \overline{\lambda}_2^2 + \overline{\lambda}_3^2 \tag{2}$$

$$\overline{I_2} = \overline{\lambda}_1^{(-2)} + \overline{\lambda}_2^{(-2)} + \overline{\lambda}_3^{(-2)} \tag{3}$$

where:

$\overline{\lambda}_1 = J^{-\frac{1}{2}}\lambda_i$, J – the total volume ratio,

J^{el} – the elastic volume ratio and λ_i are the principal stretches.

– 2nd order Polynomial form – formula (4)

$$U = C_{10}\left(\overline{I}_1 - 3\right) + C_{01}\left(\overline{I}_2 - 3\right) + C_{20}\left(\overline{I}_1 - 3\right)^2 + C_{02}\left(\overline{I}_2 - 3\right)^2 + C_{11}\left(\overline{I}_1 - 3\right)\left(\overline{I}_2 - 3\right) + \frac{1}{D_1}(J^{el} - 1)^2 \tag{4}$$

– Marlow form – formula (5)

$$U = U_{\text{dev}}\left(\overline{I}_1\right) + U_{\text{vol}}(J^{el}) \tag{5}$$

where:

U_{dev} – deviatoric part of U,

U_{vol} – volumetric part of U;

– 3rd degree Ogden form – formula (6)

$$U = \sum_{i=1}^{N} \frac{2\mu_i}{\alpha_i^2}(\overline{\lambda}_1^{\alpha_i} + \overline{\lambda}_2^{\alpha_i} + \overline{\lambda}_3^{\alpha_i} - 3) + \sum_{i=1}^{N} \frac{1}{D_i}\left(J^{el} - 1\right)^{2i} \tag{6}$$

where:

N – order of polynomial form,

μ_i, α_i – temperature-dependent material parameters.

Detailed explanation of the analytical formula can be found in [5] and discussion of the presented models in [6–9].

Obtained parameters values for Mooney-Rivlin material are relatively convergent with presented in [3]. They are equal to C_{10} = 0.0119 MPa and C_{01} = 0.7901 MPa, while parameters from [3] are equal to C_{10} = 0.0195 MPa and C_{01} = 0.8305 MPa for analysed load speed. The identified parameters of the models present good adjustment to the experimental results (Fig. 4).

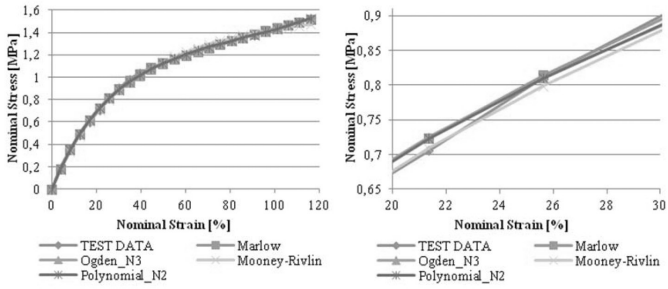

Fig. 4. Parameters identification in Abaqus 6.12, fragmentary enlarged graph on the right

4. Polymer model's verification

There has been performed a short analysis, in order to verify the polymer Finite Element Method (FEM) model as well as material models. A numerical FEM model in Abaqus 6.12 has been made for the dumbbell tensile test of the polymer PM and the determined model parameters have been used in analysis. The numerical model is characterized by following features:

– there have been used 25 600 3D elements – type C3D8H,
– only interior 8 cm of the dumbbell specimen has been modeled,
– there has been defined a displacement of boundary condition in order to compare properly calculation results with experimental test results.

The carried out calculations of the numerical model of the dumbbell specimen (for different hyperelastic models) allow determining the Cauchy stress map (Mises stress) calculated for the nominal strain ε = 30% (shown in Fig. 5). The nominal stress – nominal strain curves, also determined for the considered hyperelastic models, present good results convergence, which can be noticed in Fig. 6.

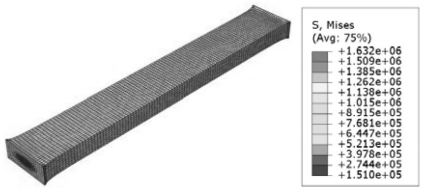

Fig. 5. Cauchy stress distribution corresponding to the nominal strain of 30% in polymer verification of the FEM model of the dumbbell specimen

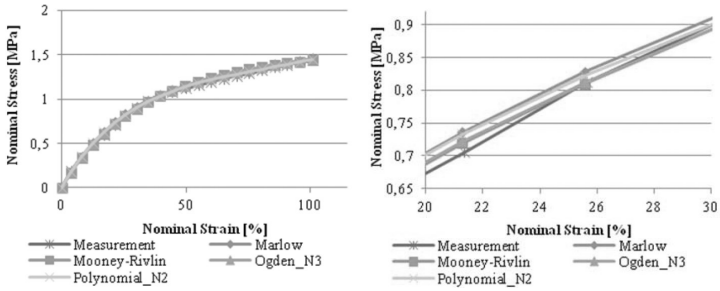

Fig. 6. Polymer model's verification, fragmentary enlarged graph on the right

The presented in Fig. 5 level of principal Cauchy stresses σ_1 (parallel to specimen's axis) can be compared with the value of the nominal stress (tensile force F divided by initial cross-section area S_0) corresponding to the nominal strain ε = 30% (Fig. 6), only after recalculation [1] according to formula (7). This comparison manifests good adjustment (comp. Fig. 5), because the nominal stress of value 0.9 MPa correspond to the Cauchy stress value of 1.17 MPa.

$$\sigma_1 = \frac{F}{S_0}(1+\varepsilon) = (0.9\ \text{MPa})\cdot(1+0.3) = 1.17\ \text{MPa} \quad (7)$$

5. PFJ numerical model description

All the numerical models of PFJ have been done using the FEM in Abaqus CAE 6.12. The dimensions and material parameters for the models have been defined in accordance with tests described above. The numerical models are characterized by following features:

– there have been used C3D8H elements for polymer and CRD8R for concrete,
– mesh density has been increased in the joint zone, specimens were modeled by 96 000 elements (for the biggest specimen),
– a contact layer has been modeled between specimen and reference rigid plane,
– there has been defined a displacement of boundary condition in order to compare properly calculation results with experimental test results. The boundary conditions were defined for rigid plane's reference points,
– concrete parameters were applied according to the carried out concrete tensile test and basing on Eurocode 2 [10]. Concrete was modeled as a linear-elastic material using parameters: $E = 32$ GPa, $\nu = 0.18$, $\rho = 2400$ kg/m^3.

6. Calculation results

There were considered 4 hyperelasic models (using the determined parameters for the dumbbell specimen) for 3 PFJ models (12 series of calculations). The obtained results for various hyperelastic models, calculated for the specimens presented in Fig. 2, are compared in Fig. 7 with the experimental data of the PFJ specimens. It can be noticed that the adjustment of the numerical analysis and laboratory test data is not very well.

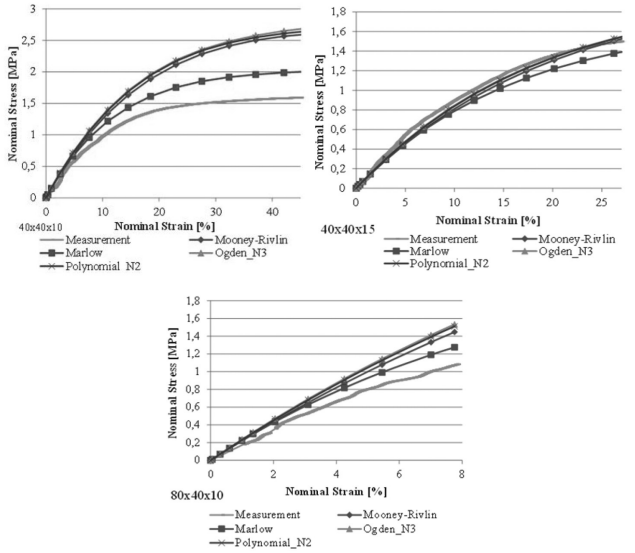

Fig. 7. Comparison of the numerical and laboratory tests results for $40 \times 40 \times 10$ (upper left), $40 \times 40 \times 15$ (upper right) and $80 \times 40 \times 10$ (bottom) PFJ variants

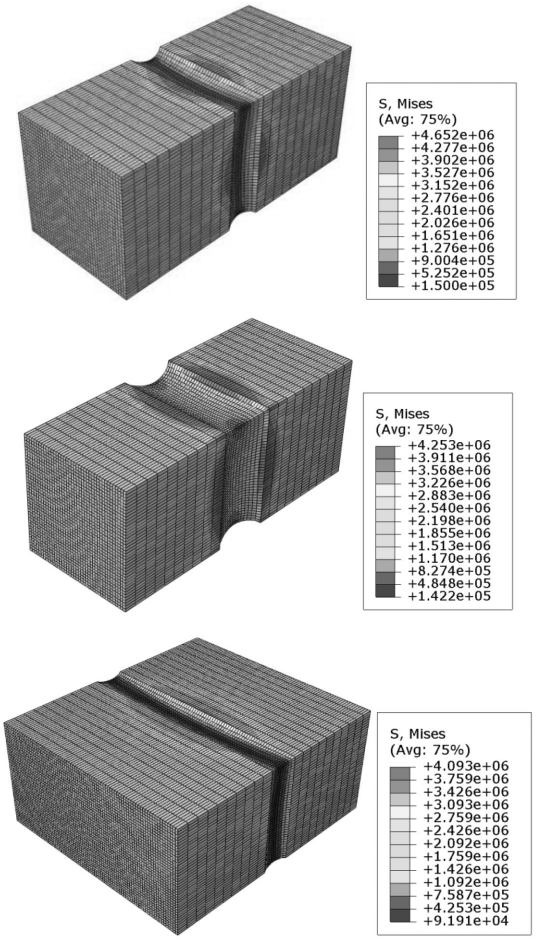

Fig. 8. Stress distribution for models with particular dimensions and nominal strain: $40 \times 40 \times 10$ and 30% (at the top), $40 \times 80 \times 10$ and 30% (in the middle), $40 \times 80 \times 10$ and 24% (at the bottom)

The calculated results for the PFJ models allowed also presenting maps of stress distribution in the considered models of the flexible joints, working under tensile stress (Fig. 8). It can be noticed that in the case of large deformations the stress distribution is complex and not evenly distributed at the interface between the concrete substrate and the polymer joint. It confirms also comparison of the stress distribution in the particular cross-section layers of the polymer PM (Fig. 9). In the middle layer, the stress is almost evenly distributed over the whole surface (with low intensity). On the other hand in the interface layer, peaks of stress concentrations (of high intensity) occur at the edges of the cross-section, whereas in the middle of the cross-section the stress is of low intensity. This conclusion was also confirmed by analysis presented in [1].

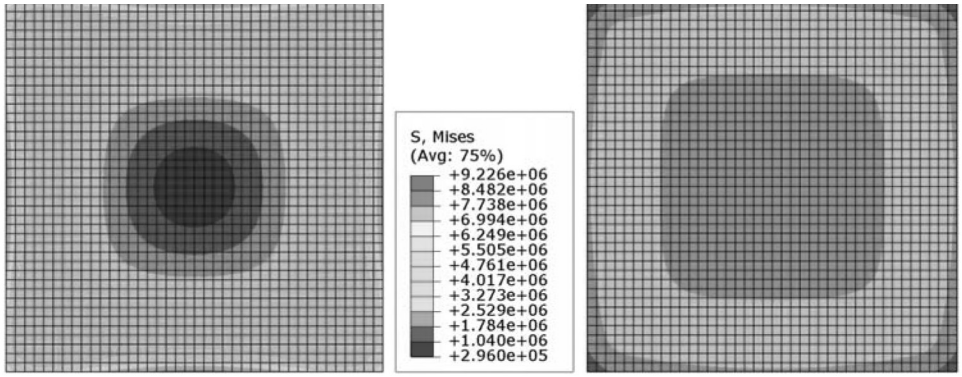

Fig. 9. Stress distribution in polymer layer at the interface between polymer and concrete (on the left) and in middle of the polymer layer cross-section (on the right)

6. Conclusions

Basing on the presented results following conclusions can be drawn:

- the hyperelastic material models, obtained during the uniaxial dumbbell tensile test is adequate for tensile calculations of a specimen made of polymer. However, using the same model in the PFJ calculations it leads to inaccuracies of about 30% or more,
- there is a big influence of the hyperelastic model type on results convergence; basing on this analysis it can be found that the Marlow form leads to smaller inaccuracy in analysed cases,
- both dimensions of specimens cross-section and polymer layer thickness influence the results' discrepancy. In presented example the highest convergence was obtained for specimen $40 \times 40 \times 15$, while for other specimens numerical models are characterized by a greater connection stiffness. At this point it is difficult to explain those results,
- laboratory as well as numerical test results lead to conclusion, that polymer's behaviour in the PFJ tensile test is more rigid than in the dumbbell one; the rigidity increase can be connected with complex stress state as well as shear effects in polymer layer next to the concrete surface,
- the pure adjustment of the PFJ model to the experiment results can be also connected with rheological behaviour, not included in these analyses.

This work indicates that PFJ theoretical model as well as numerical approach should be developed. As a continuation of this work, further laboratory tests as well as theoretical and numerical research will be performed in order to describe correctly the PFJ mechanical behaviour, including also rheological aspects.

References

[1] Kwiecień A., *Polimerowe złącza podatne w konstrukcjach murowych i betonowych*. Monografia nr 414, Wydawnictwo Politechniki Krakowskiej, Seria Inżynieria Lądowa, Kraków 2012.

[2] Kwiecień A., Gruszczyński M., Zając B., *Tests of flexible polymer joints repairing of concrete pavements and of polymer modified concretes influenced by high deformations*, Key Engineering Materials Vol. 466 (2011), Trans Tech Publications 2011, 225-239.

[3] Kwiecień A., Kuboń P., Zając B., *Experimental verification of hyperelastic model of polymer on a case study of the flexible polymer joint*, Zeszyty Naukowe Politechniki Rzeszowskiej nr 276. Budownictwo i Inżynieria Środowiska, Zeszyt 58 nr 3/2011/II, 373-380.

[4] PN-EN ISO 527-1: 1998 *Tworzywa sztuczne – Oznaczanie właściwości mechanicznych przy statycznym rozciąganiu – Zasady ogólne*.

[5] Abaqus Theory Manual, Abaqus On-line documentation, http://baribal.cyf-kr.edu.pl:2080/v6.7

[6] Weber G., Anand L., Finite deformation constitutive equations and a time integration procedure for isotropic, hyperelastic-viscoplastic solids. Computer Methods in Applied Mechanics and Engineering, 79 (1990), s. 173–202.

[7] Kaliske M., Rothert H., *On the finite element implementation of rubber-like materials at finite strains*. Engineering Computations14, 1997, 2, 216–232.

[8] Aidy A., Hosseini M., Sahari B.B., *A review and comparison on some rubber elasticity models*, Journal of Scientific and Industrial Research, 69, 2010, 495-500.

[9] Jemioło S., *Studium hipersprężystych własności materiałów izotropowych: Modelowanie i implementacja numeryczna*, Prace naukowe, Budownictwo, OWPW, Warszawa 2002.

[10] Ajdukiewicz A., *EUROKOD 2. Podręczny skrót dla projektantów konstrukcji żelbetowych*, Stowarzyszenie Producentów Cementu, Kraków 2009.